Citation for published version:
Storey, JP, Hammond, JL, Graham-Harper-Cater, JE, Metcalfe, BW & Wilson, PR 2016, Modelling Dynamic Photovoltaic Arrays for Marine Applications. in Control and Modeling for Power Electronics.

Publication date:
2016

Document Version
Peer reviewed version

Link to publication

Publisher Rights
Unspecified

University of Bath

General rights
Copyright and moral rights for the publications made accessible in the public portal are retained by the authors and/or other copyright owners and it is a condition of accessing publications that users recognise and abide by the legal requirements associated with these rights.

Take down policy
If you believe that this document breaches copyright please contact us providing details, and we will remove access to the work immediately and investigate your claim.

Download date: 13. May. 2019

Modelling Dynamic Photovoltaic Arrays for Marine Applications

Jonathan P. Storey, Jules L. Hammond, Jonathan E. G-H-Cater, Benjamin W. Metcalfe, and Peter R. Wilson
Department of Electronic & Electrical Engineering, University of Bath, Bath, BA2 7AY, UK.

***Abstract*—This paper presents a new simulator platform with findings from experiments aiming to identify the electrical characteristics of a marine vessel covered in photovoltaic modules, operating in various sea conditions. More specifically, we show that by giving a solar array the ability to reconfigure the arrangement of its modules in real time, that significant improvements (up to 50%) in power yield can be achieved compared to typical static arrays. A bespoke MATLAB simulator has been developed in order to model the complex interplay between the electrical arrangement of photovoltaic modules, the position of the photovoltaic modules on the vessel, the vessel's tilting motion on the surface of the sea and the resultant irradiance based on the position of the Sun in the sky. Our approach allows the user to define these factors using a simple and intuitive graphical user interface so that a range of scenarios can be quickly simulated. We have used a basic test strategy that allows us to measure the effectiveness of different arrays and quantify performance in terms of mean output power and power stability over a range of sea conditions. A key factor in the effectiveness of the use of marine survey vessels is their ability to remain at sea for extended periods, preferably avoiding the use of high-carbon fuel sources such as diesel generators. This is of particular importance when observing marine life as the platform needs to operate as quietly as possible. The ASV Global C-Enduro autonomous, self-righting platform is the initial application for this new energy harvesting system, with the aim to extend mission endurance. A second case study has also been performed in parallel with this, using a much more divergent orientation of onboard photovoltaic modules in order to asses the ability for a dynamic photovoltaic array to increase and stabilise power output.**

***Index Terms*—Dynamic Photovoltaic Arrays, Reconfigurable Photovoltaic Array, Irradiance Profiling, ConfigArray**

I. Introduction

It is quite common for marine survey platforms to use some form of photovoltaic (PV) array to provide power to the vessel. The ASV Global C-Enduro shown in Figure 1 has twelve 100 W PV modules arranged in a static 4×3 array, as well as a wind turbine to generate electricity. There is a specific issue for marine systems where the system is highly dynamic (i.e. the panels on the vessel are subject to insolation variations with respect to the sea conditions), and there are also partial shading issues from spray, salt deposits over extended periods and other detritus from sea birds, weed and algae. These can all cause a degradation on a marine-based PV array, leading to effective partial shading on a short- and long-term basis.

Using a static solar array (similar to a domestic rooftop PV installation) has a significant disadvantage when a module is subject to irradince variations, in that the effect of partial

Fig. 1: The autonomous C-Enduro platform from ASV Global.

shading can dramatically reduce the overall power output from the array, even though most of the individual modules may be receiving high levels of irradiance from the Sun. Modern dynamic photovoltaic arrays (DPVA) are one approach to address the issue of partial shading and irradiance mismatch, differing from static PV arrays by being able to reconfigure the module interconnections in real time to create a configuration that will provide maximum power output for that given moment. There are several approaches that have been developed to improve the power output from a PV array including the Irradiance Equalised DPVA (IEq-DPVA) [1], [2], the Adaptive Bank DPVA (AB-DPVA) [3], and the Optimised String DPVA (OS-DPVA) [4]. The most versatile of these systems is the irradiance equalized DPVA as it allows for any configuration to be implemented and has the ability to balance any module mismatch seen. In order to utilise this method, the array must be arranged in a Total Cross Tied (TCT) topology and the most poignant feature of this type of architecture is that the power output from all modules in the same tier (or row) are summed together because they are effectively in parallel.

In order to analyse how to best control the dynamic array, a simulator is needed so that repeatable test cases and various scenarios of shading can be applied. The core features of the simulator have been previously discussed [5], however in this project we have advanced this 'snapshot' simulator so that it is now possible to calculate the IV characteristics of an

array over a period of time. With a temporal dimension it is possible for each module to have an irradiance sequence that continuously evolves. Here we have used this ability to program environments expected from the vessel at sea, operating in highly dynamic sea conditions. The simulator will link to a hardware power electronics hub that can be directly controlled either by an onboard ARM processor or from the simulator (using hardware in the loop) via a serial link. This allows characterisation of the system, pre-configuration optimisation and simulation analysis.

II. Dynamic Array Topologies and Methods

There are several classfications of dynamic array that can be used to remove the effects of irradiance mismatch and each of these can have specific operating modes and sorting algorithms. The simplest dynamic array is a fixed configuration DPVA [6] and it is noted for its ability to reconfigure into a select few arrangements. This type of array is particularly poor at resolving issues with shading as it is unable to effectively manoeuvre the modules around chaotic scenes. The next type of dynamic array is known as the string configured DPVA [7] and in its most versatile form, it is highly adaptive and could yield significant improvements in the uncertain environments that we are considering here. However, it has several notable drawbacks, namely that it is difficult to control and the string-like topology does not allow for irradiance mismatch balancing. In contrast to this, the most versatile TCT dynamic photovoltaic arrays (TCT-DPVAs) are able to almost completely remove the effects of irradiance mismatch. They achieve this by sharing the current burden between each module within a tier, and therefore average the power generation across the array. This feature needs to be managed appropriately in order to gain maximum benefit.

A. The Irradiance Equalised TCT-DPVA

Before discussing how best to control the dynamic array, it is prudent to briefly analyse how the TCT architecture works. Referring to Figure 2, the first thing to note is the high-level topology where all modules in a tier are connected in parallel with a busbar. This interconnection allows for all the modules within the tier to feed current to the bus independently of one another and this effect has been noted in literature [8]. From an electrical point of view, it means all modules must share the same voltage but they can provide different currents. This is favourable as photovoltaic modules are primarily current sources, resulting in strong modules producing an excess current supporting weak modules producing less current. These tiers are then connected in series and the current through the string is now dependant on the weakest of the tiers. As will be shown, this approach of parallel first and series second is what makes this structure so competent at resolving module mismatch and it is central to the principles of irradiance equalisation through dynamic reconfiguration. In contrast, the Series Parallel (SP) topology will, as its name suggests, arrange the modules in the opposite fashion.

An example of how reconfiguring within a TCT removes the effects of partial shading is shown in Figures 2 and 3. In Figure 2 the bottom tier is collectively producing 350 W of power, the middle tier is producing 400 W and the top tier is producing 450 W. As each of these tiers are in series, the same current must be drawn through all of them. In this configuration the bottom tier is the weakest and it imposes a limit on the amount of current that can be drawn. If the load tries to draw more, then the voltage from this part of the array will collapse. In effect, all the tiers are being forced to extract only 350 W each (totalling 1050 W) even though the array can potentially provide 1200 W.

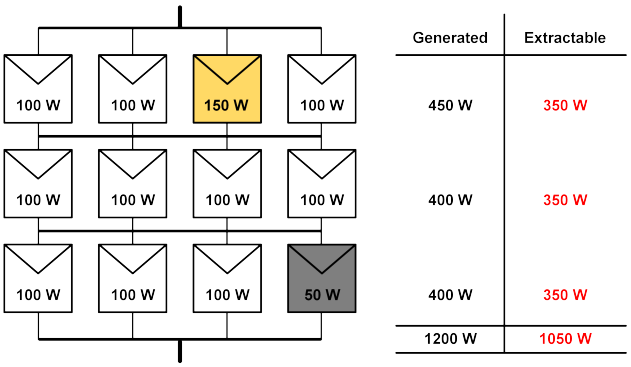

Fig. 2: Impact of partial shading on PV modules before reconfiguration.

In Figure 3, two of the modules have been electrically repositioned using the switch matrix (the modules remain physically static) and under this new configuration, every tier produces 400 W. As all tiers are producing an equal amount of power, the full 1200 W can be extracted. This is a simplified example of irradiance equalisation but it highlights the concept. In a real system, each module will have a non-exact irradiance value that can vary continuously over time.

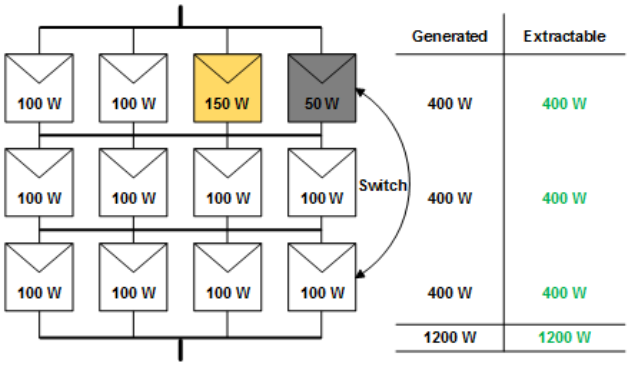

Fig. 3: An example of the reconfiguration of a TCT-DPVA to improve power extraction.

There are many examples of switch matrices that can reconfigure modules in the literature, but the one which provides

the most flexibility is shown in Figure 4. Here a single module has a number of bidirectional switches connected to both its positive and negative terminals and they allow for the power source to be connected to any of the tiers. The total number of ways to utilise these switches is described by the equation $N = 2^n$, where an array that has eight switches (n) per module (i.e. three tiers) has a total 256 switch positions (N) but only a few of these are electrically useful. For the basic system being discussed here, there are only four switch positions that are of interest. Now that we have identified how the DPVA is able to locate any module within its tier, we will now discuss the marine environment model.

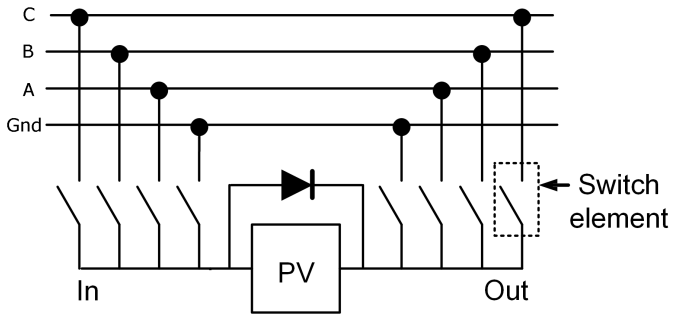

Fig. 4: Example showing a PV module connected to a switch network comprised of eight switches.

III. Modelling Marine Vehicles in Active Environments

The simulator has been designed with three basic aspects in mind, the first being the generation of IV characteristics for the modules in the array, which is discussed in the next section. The C-Enduro platform uses Solbian 100 W flexible SP100 modules, the key parameters such as open circuit voltage, short circuit current, diode characteristics and nominal power (as well as other parameters) are entered using the user interface. Next the geometry of the vessel is mapped inside a three dimensional domain where its angular position can be arbitrarily rotated while an irradiance source emanating power from any position above is rendered. This powerful combination of vessel curvature, movement and relative source position means that any shape can be supplied as an input and all possible angles of incidence can be simulated. The last property of the simulator is its ability to chart the evolution of these parameters and their effects over time. Including this additional dimension means it can compute the four dimensions required to effectively emulate the experiences of the vessel in real life.

A. Creating the Boat Frame

The first new feature that the simulator incorporates is the ability to define the shape of the frame that the PV modules are attached to. To do this, each module has a static pitch and roll value assigned to it when it is created, where this default orientation is caused by the geometry of the frame. The angles are considered relative to the vertical axis and because in most cases an array has all modules facing the same direction, it is normal for these offset values to be the same (i.e. all panels on a roof have the same orientation). This is not necessarily the case with arrays attached to vehicles as it is likely that the chassis will have curves and contours that the modules must adhere to. Figure 5 shows an example geometry that is used later in conjunction with the C-Enduro geometry in order to yield comparative results from the test sequences presented in Section V. Each module has some inherent pitch and roll value relative to the horizontal plane, for example module A1 has a -25 degree roll and a -20 degree pitch. Table 1 has the full listing of PV module tilt values for both the modelled geometries. Equation 1 describes how the angle of incidence attenuates power as a function of the Sun's altitude angle (α) and then the module's tilt (β) when variation happens in one dimension (i.e only changes in roll). Similarly, Equation 2 describes the attenuation of incident power when considering both pitch and roll.

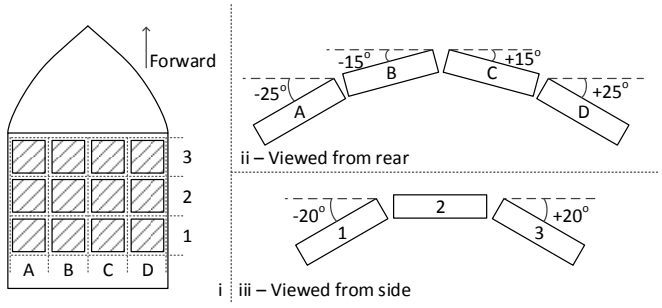

Fig. 5: Diagram showing the modified panel arrangement used in later simulations.

$$P_{module} = P_{incident}\big[(Sin(\alpha + \beta)\big] \quad (1)$$

$$P_{module} = P_{incident}\big[Sin(\alpha + \beta_{pitch}) \times Sin(\alpha + \beta_{roll})\big] \quad (2)$$

B. Specifying the Boat Motion

The next new feature added to the simulator is the ability to define sea conditions over a period of time and therefore the vessel's real movement in terms of pitch and roll with respect to the vertical axis. Specifically, the user must input the maximum tilt angles expected by the vessel in degrees. For simplicity, it is assumed that the vessel will oscillate between plus and minus the maximum tilt in a sinusoid without decaying. The user can also set the frequency of the oscillations and the phase between the two axes of motion.

In order to illustrate how the angle of incidence is affected by the motion, consider the simplified one dimensional scenario in Figure 6. It shows a cross section of a hull at three moments within the roll sequence. Equation 1 is used to find the incident irradiance on each module surface given its

TABLE I: Table outlining the specific tilt angles of each module in the two modelled topologies.

	C-Enduro		Modified	
Module #	*roll*	*pitch*	*roll*	*pitch*
1	5	−5	−25	20
2	−5	−5	−15	20
3	−5	−5	15	20
4	5	−5	25	20
5	−5	5	−25	0
6	−5	5	−15	0
7	5	5	15	0
8	5	5	25	0
9	−5	0	−25	−20
10	0	0	−15	−20
11	5	0	15	−20
12	0	5	25	−20

effective roll relative to the Sun's rays, which are assumed to be coming from directly overhead.

At the first moment ($t1$) the vessel is rolled -20 degrees and this tilt couples with each module's static tilt to give rise to the actual angle of incidence seen from each module. For module A, both the static roll (-25) and the vessel roll (-20) act constructively to give a full roll angle of -45 degrees. This means the module will perform poorly as the incident power on its surface is attenuated considerably. Conversely, module D has a positive static roll ($+20$) and a negative boat roll (-25), resulting in an angle of incidence of -5 degrees perpendicular to the Sun. As this module is almost directly facing the Sun, it will generate close to maximum power. In the next moment ($t2$), the vessel is flat in the water and modules A and B see a rising power characteristic during this transition, while modules C and D see a falling power characteristic.

This example highlights one of the main advantages of being able to simulate an environment over time: It allows for the evolution of irradiance to be observed and this allows for the testing of new types of switching mechanisms and algorithms that rely on a history of events.

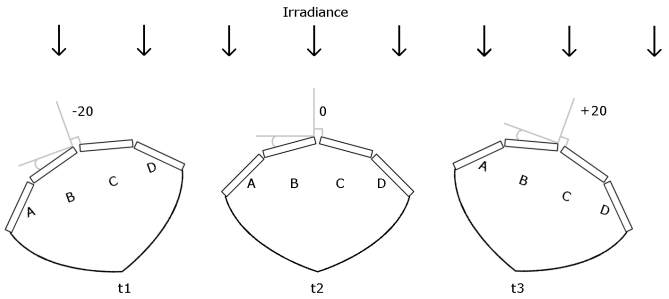

Fig. 6: Single axis demonstration of irradiance effects with roll

C. Identifying Module Azimuth Considering the Apparent Yaw

So far we have defined the pitch and roll of the modules relative to the boats frame, and the frames motion in the water. In order to calculate the irradiance across the modules surface, the azimuth relative to the Sun must now be found.

To simplify the model, the effects of roll and pitch on the azimuth were assumed to be independent to one another. The azimuth was therefore found by calculating the polar form of the applied pitch and roll angles.

The altitude is measured relative to the original pitch–roll plane, meaning that the influence of roll on subsequent pitches must be considered. This poses an interesting property of three dimensional geometry, where the pitch is mapped onto an apparent yaw as a direct result of the previously applied roll. This artefact of Euler angles is well understood and at the extreme case where a 90 degree roll is applied, all changes in pitch will map directly to changes in the boat's azimuth relative to the Sun. It should be noted that this apparent change in yaw does not reflect a change in heading for the simulated boat, but rather is a direct artefact of the boats tilting motion. Equation 3 must therefore be used to find the resultant altitude (β).

$$\beta = Cos^{-1}\big[Cos(pitch) \times Cos(roll)\big] \tag{3}$$

D. Identifying Angle of Incidence in 3D

This situation becomes slightly more complicated when all three dimensions are included. The first thing to be aware of is both the Sun and the module surface now have an azimuth value as well as a altitude. This means the number of terms has gone from two to four, where the Sun's position in the sky is now described by its altitude angle (α) and its azimuth angle (θ), and similarly the modules now have an altitude angle (β) and a module azimuth (ϕ). The general equation for finding the incident irradiance on a module surface in three dimensions is shown in Equation 4 and in normal situations the module altitude and azimuth are fixed (usually to a roof) while the Sun moves slowly according to the time of day. However, as the modules we are interested in are attached to a fast-moving platform, it appears the other way around and it is the modules' altitude and azimuth that are moving and the Sun appears to be static in the sky. As usual, North is defined as 0 degrees with increasing values measured clockwise towards the East.

$$P_{module} = P_{incident}\big[Cos(\alpha) \times Sin(\beta) \times Cos(\phi - \theta) + Sin(\alpha) \times Cos(\beta)\big] \tag{4}$$

IV. The Simulation Environment

A simulation environment has been programmed into MATLAB and it enables repeatable and bespoke tests to be conducted while allowing the modification of the parameters governing physical phenomena in conjunction with observing the effects of tuning the control strategy. The analysis of the results revealed that a dynamic PV array can provide improvements up to 50% compared to a static array in the

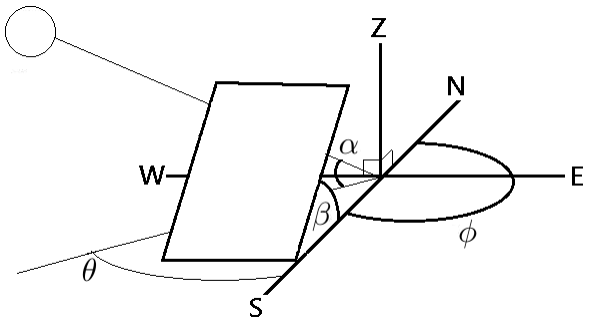

Fig. 7: A panel facing South with an azimuth ϕ and an altitude β. Showing the Sun with a westward azimuth θ and an altitude α as measured from the horizon.

worst-case scenario. A full disclosure of the test strategy and the test results are discussed in the next section. As an overview, the simulator will calculate the mean power output from a range of different array types situated atop a boat deck. As mentioned before, it takes into account features of the vessel's physical geometry and the interaction with its movement such that it gives an insight into the irradiance profile cast upon a moving vessel.

A. The Simulator Interface

The graphical user interface has been designed so that the user interacts with a windows style main menu which guides them through the required steps prior to conducting a simulation. The details about the solar array, the boats movement in the water and the Sun's location are entered first. Next the typical physical parameters for solar cells are entered by the user, these include variables such as the series resistance (R_{series}), shunt resistance (R_{shunt}), cell efficiency (μ), cell area [cm^2], the cell's maximum power point (V_{mpp}), number of cells per module, the saturation current and the diode ideality factor. With this information acquired, the user can then perform a simulation, which renders an IV curve of each module at each time step, for the period of simulation. Once the simulation is complete, the user can interrogate the modules by observing an animation depicting the evolution of its IV characteristic as the boat moves. A second notable animation shows the overall mean power output of all modules simultaneously and therefore gives the user immediate indication of the influence of the frame's geometry and boat movement across the array as a whole.

Now that the simulator has rendered each module's IV profile over the time period, the user can then either arrange the modules in a configuration of their choice, or they can let a sorting algorithm perform a number of reconfigurations at specific moments within the simulated period. The user can implement any sorting algorithm they wish to identify an optimum configuration and they can also implement various trigger mechanisms that instigate the reconfigurations. For the work presented here, the simple Best-Worst algorithm was used to identify an optimised arrangement and the reconfiguration procedures where triggered when the boat's tilt values exceeded specific points. This was deemed a suitable method for identifying when a reconfiguration was required as it directly relates the triggering to changes in irradiance as seen from the modules' surface. Furthermore, this could easily be implemented in a real system by using an accelerometer to indicate changes in either pitch or roll.

B. Modelling Photovoltaic Cells

The method for calculating the modules' IV curves has been previously fully discussed in [5], but as an overview, it subtracts the result from the single diode model from the approximate short circuit, described by Equations 5 and 6 respectively, where n is the ideality factor, k is the Boltzmann constant and T is the temperature in Kelvin. Intuitively this is what happens inside the solar cell, where a fixed current is being produced by the irradiance and any current not drawn through the terminals flows through the internal diode.

$$I_{sc} \approx \frac{P_{area} \times \mu}{V_{mpp}} + \frac{V_{mpp}}{R_{shunt}} \tag{5}$$

$$I_{diode} = I_0\Big\{exp\Big[\frac{q(V + IR_s)}{nkT}\Big] - 1\Big\} + \frac{V + IR_s}{R_{shunt}} \tag{6}$$

As Equation 6 is transcendental (i.e. it has terms for current on both sides) it must be rewritten as shown in Equation 7 where the parameters are chosen to force the result to zero. For the simulation platform presented here, the voltage parameter (V_{step}) is recursively set to one of a sequence of equidistant values (i.e. from 0.o V to 1.0 V in steps of 0.1 V) and MATLAB's zero finding function is used to find which current (x) will cause the equation to resolve to zero. The result is two synchronised vectors, that describe the current flow through the internal diode for given voltages. These diode currents are subtracted from the approximated short circuit current to successfully render the IV curve of the solar cell. As this exercise is purely mathematical, it can yield results that do not exist in real life. For instance, the numbers may suggest a diode current that is higher than the generated short circuit current. Obviously this cannot happen, so the next step is to remove all values below zero.

$$0 = I_0\Big\{exp\Big[\frac{q(V_{step} - xR_s)}{nkT}\Big] - 1\Big\} + \frac{V_{step} - xR_s}{R_{shunt}} \tag{7}$$

The final step in the simulation is to add bypass diodes to each module. It is required by the simulator as it allows for all modules to pass the same current, even though they may not generate the same short circuit current due to differences in irradiance. Essentially, it will append a second IV characteristic to the first IV curve, but this time it will have a negative voltage of around 0.6 V as shown in Figure 9.

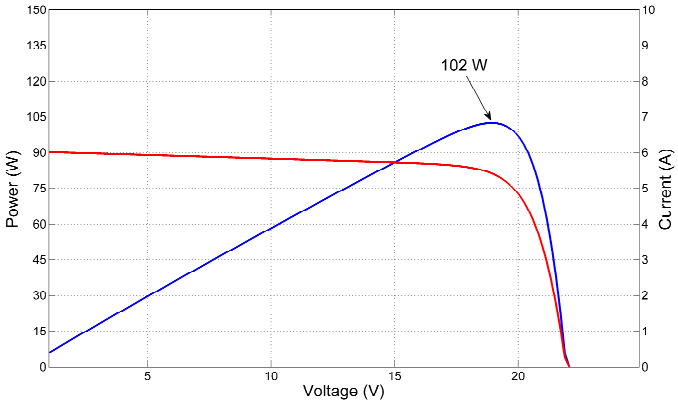

Fig. 8: Results of a simulation for the Solbian 100 W modules used on the C-Enduro. Maximum power of 102 W, with an I_{sc} of 6 A and V_{oc} of 22 V

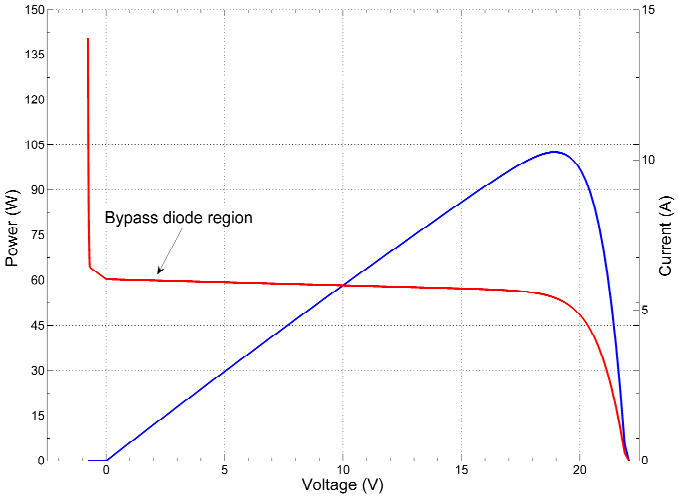

Fig. 9: Each module must have a 'bypass diode' so that modules under different irradiances can still carry the same current.

V. Test Cases

Two different panel arrangements were investigated, the first arrangement is that of the ASV Global C-Enduro vessel which has completely flat or modest tilt angles ($<$ 5 degrees). A second, modified arrangement, consisting of a 4 $\times$ 3 array with symmetry across both the x and y planes was also modelled with more aggressive tilt values ($\leq$ 25 degrees) in order to demonstrate how a DPVA system can cope with the greater module deviations (see Figure 5). In both cases the following PV cell parameters were used: 300 K operating temperature; 200 fA diode saturation current; 1.83 diode ideality factor; 1 Ω series resistance (R_s); 1000 Ω shunt resistance (R_{shunt}); 0.57 V maximum power point voltage (V_{mpp}); 18.4% efficiency; 12.55 cm^2 area, 32 series cells per module; and a nominal irradiance of 1000 Wm^{-2}.

The tilting action of the vessel due to varying sea conditions has been controlled using two individual sinusoids for pitch and roll. In all the following scenarios we have modelled a wave approaching the vessel at an angle of 45 degrees. Given that a vessel is often longer than it is wide, we have set the amplitude of the pitch to be half that of the roll. This allows us to define the effect of the sea condition on the vessel using the single parameter, 'maximum tilt'. As an example, a maximum tilt of 10 degrees would relate to a maximum roll of 10 degrees and a maximum pitch of 5 degrees over a period. The first test was to show the differences between the SP, TCT and DPVA architectures with the Sun in a position of *equiumbra*, that is 45 degrees altitude (0 degrees azimuth).

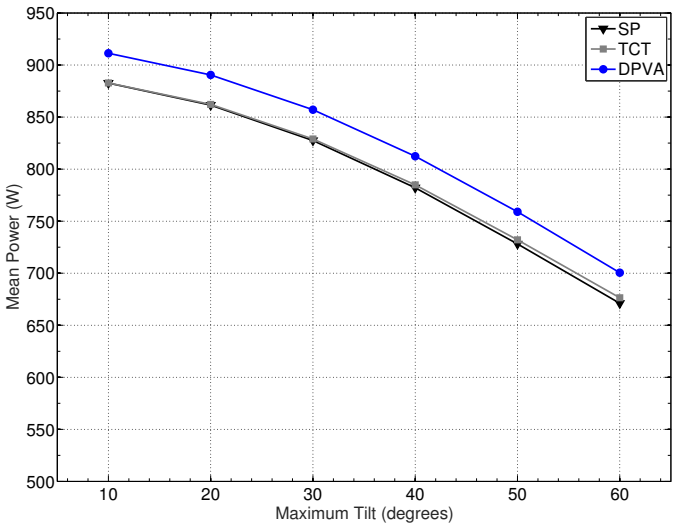

Fig. 10: Results for the ASV Global C-Enduro system at 45 degrees altitude and 0 degrees azimuth.

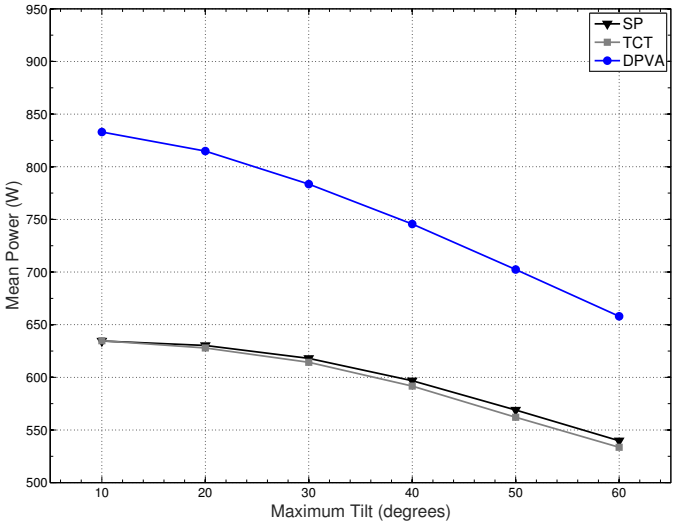

Fig. 11: Results for the modified system at 45 degrees altitude and 0 degrees azimuth.

For both systems we can see that a DPVA outperforms both static SP and TCT architectures across all modelled sea conditions. In the modified panel arrangement the static SP

and TCT architectures struggle to balance the large variances in power that the more aggressively tilted panels generate. This expected result confirms that the DPVA architecture is able to cope with both tilted panels and varying sea conditions, producing significantly increased mean power (up to 31%) compared to SP and TCT architectures. A point to note is that in these two scenarios, both the static architectures respond similarly. In the case of the C-Enduro topology the static TCT architecture appears to slightly outperform the static SP architecture. For the modified topology this behaviour is reversed. The effect of the Sun's altitude was then simulated, with altitude decreasing from 90 degrees to 15 degrees in steps of 15 degrees. Azimuth was kept constant at 0 degrees, whilst the maximum tilt of the vessel caused by the sea conditions was investigated from 10 to 60 degrees in 10 degree steps. A percentage difference versus the best performing static architecture was then calculated for data presentation (Figure 12).

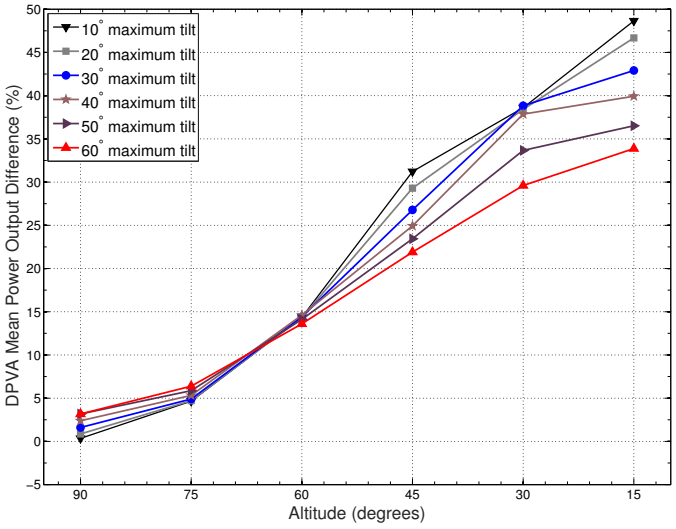

Fig. 12: Results showing the DPVA output performance through varying Sun altitude values with differing sea conditions for the modified toplology.

Here it can be seen that a DPVA architecture produces significant improvements in power yield over the next best static architecture. As the Sun decreases in altitude (from the zenith to the horizon) the improvement over the static architectures increase considerably. With the Sun low in the sky, at an altitude of 15 degrees, the DPVA architecture produces an increase in output power of 34% to 49% depending on the simulated sea condition. The final stage was to then investigate how the azimuth angle of the Sun affected the system. We decided to fix the Sun's altitude at a value of 45 degrees and then increase the Sun's azimuth from 0 to 90 degrees, essentially pivoting the Sun around the vessel. Again a range of maximum tilt values were modelled and a percentage difference between the DPVA architecture and the next best performing static architecture calculated.

Interestingly as the Sun moves around to 75 degrees azimuth

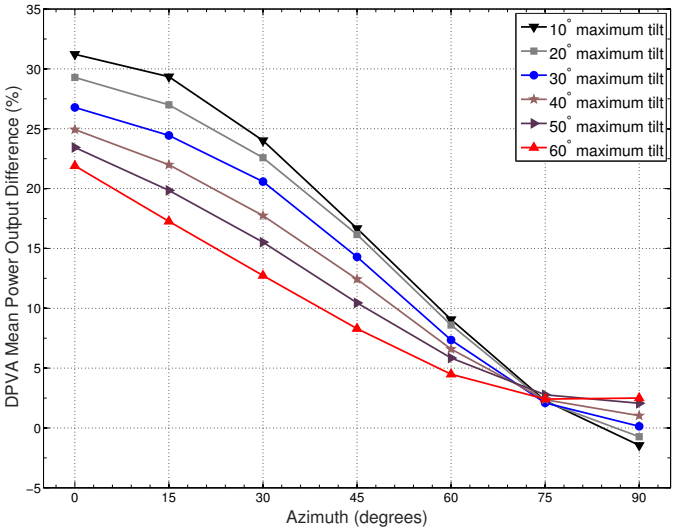

Fig. 13: Results showing the DPVA output performance through varying Sun azimuth angles with different sea conditions with a fixed Sun altitude of 45 degrees for the modified topology.

the percentage difference of the DPVA performance versus the next best static architectures almost converge to around 2.5%, regardless of the sea condition. We believe this to be a specific result of the array topology with respect to the Sun's position in the sky creating a symmetry whereby the tilting motion of the vessel imposes minimal changes in effect. As the azimuth increases further to 90 degrees, the DPVA architecture actually produces less power compared to the static SP and TCT architectures at maximum tilt values less than 30 degrees. We believe this to be caused by a combination of attributes: the asymmetry in the 4×3 array, the limited tilting motion (that would otherwise aid in averaging the irradiance) and the simplistic approach of the Best-Worst algorithm.

VI. Conclusions

This paper has presented a bespoke simulator created in MATLAB that allows the effects of the Sun's position in the sky as well as a vessel's dynamics caused by sea conditions to be analysed. Such a system can be used to design optimised panel arrangements based on a given marine environment for a range of PV architectures. Furthermore the ability for a DPVA to account for aggressive panel tilts in a range of Sun altitude and azimuth angles has been demonstrated using a simple Best-Worst algorithm. The use of tilted modules allows increased panel surface area for a given deck area, providing an increased payload volume under the panels, as well as the ability to conform to any packaging restrictions imposed by the vessel itself. It is envisaged that a DPVA controlled using a more intelligent algorithm such as an arbitrary tier resizing algorithm would yield further gains, particularly with asymmetric arrays that can suffer from the heavily unbalanced distributions of irradiance caused by their orientation in relation to the position of the Sun. Other aspects

that we plan to incorporate is the albedo contribution caused by the Sun's reflection on the sea surface and the effect of shading caused by the vessel structures.

REFERENCES

[1] G. Velasco-Quesada, F. Guinjoan-Gispert, R. Piqué-López, M. Román-Lumbreras and A. Conesa-Roca, "Electrical PV Array Reconfiguration Strategy for Energy Extraction Improvement in Grid-Connected PV Systems," *IEEE Trans. Ind. Electron.*, vol. 56, no. 11, pp. 4319-4331, Nov. 2009.

[2] J. Storey, P.R. Wilson, and D.M. Bagnall, "Improved optimization strategy for irradiance equalization in dynamic photovoltaic arrays," *IEEE Trans. Power Electron.*, vol. 28, no. 6, pp. 2946-2956, June 2013.

[3] D. Nguyen and B. Lehman, "An Adaptive Solar Photovoltaic Array Using Model-Based Reconfiguration Algorithm," *IEEE Trans. Ind. Electron.*, vol. 55, no. 7, pp. 2644-2654, July 2008.

[4] J. Storey, P.R. Wilson, and D.M. Bagnall, "The Optimized-String Dynamic Photovoltaic Array," *IEEE Trans. Power Electron.*, vol. 29, no. 4, pp. 1768-1776, Apr. 2014.

[5] J. Storey, T. Redman, P. Wilson and D. Bagnall, "Integrated simulator and hardware platform for dynamic photovoltaic array optimization and testing." *J. Nanoelectron. Optoelectron.*, vol. 10, no. 1, pp. 104-110, 2015.

[6] Z.M Salamehand and F. Dagher, "The effect of electrical array reconfiguration on the performance of a PV-powered volumetric water pump," *IEEE Trans. Energy Convers.*, vol. 5, no. 4, pp. 653-658, Dec. 1990.

[7] M.A. Chaaban, M. Alahmad, J. Neal, J. Shi, C. Berryman, Y. Cho, S. Lau, H. Li, A. Schwer, Z. Shen, J. Stansbury and T. Zhang, "Adaptive photovoltaic system," *IECON 2010 - 36th Annual Conference on IEEE Industrial Electronics Society*, Glendale, AZ, 7-10 Nov. 2010, pp. 3192-3197.

[8] L. Gao, R.A. Dougal, S. Liu and A.P. Iotova, "Parallel-Connected Solar PV System to Address Partial and Rapidly Fluctuating Shadow Conditions," *IEEE Trans. Ind. Electron.*, vol. 56, no. 5, pp. 1548-1556, May 2009.